

Supporting information

Crystal and electronic structure manipulation of Laves intermetallics for boosting hydrogen evolution reaction

Dong Zhang^a, Shen-Jing Ji^a and Nian-Tzu Suen^{a,*}

^a College of Chemistry & Chemical Engineering, Yangzhou University, Yangzhou 225002, China

*Corresponding author: Nian-Tzu Suen (006641@yzu.edu.cn)

Experimental Section

Chemical reagents and synthetic method. Praseodymium powder (99 %), Terbium powder (99 %), Yttrium ingot (99.9 %), Erbium powder (99.9 %) and Ruthenium powders (99.9 %) used in this work were purchased from Ming-Ling chemical company. Other chemicals such as Cobalt sheets (99.5%), Pt/C (loading 20 %) and KOH (ACS grade) were acquired from Aladdin chemical company. These materials were used as received without purification and were stored in an argon-filled glovebox to prevent the possible oxidation on the surface of raw materials due to the oxygen and moisture in air. Laves intermetallics ($RECo_2$ and $RERu_{0.5}Co_{1.5}$ ($RE = Pr, Tb, Y$ and Er)) can be synthesized by reacting corresponding elements directly with arc-melting technique. For instance, to synthesize $PrCo_2$, one first weighted Praseodymium powder and Cobalt sheet based on the stoichiometric ratio (1 : 2), and the total amount of the raw materials is close to 1 g. These raw materials were then placed on copper substrate inside a custom-designed arc melting furnace and the furnace chamber was evacuated and purged with argon gas (99.999 %). This purging process was repeated three times to lower the oxygen level in case of sample oxidation and the argon pressure of the chamber was set at 380 torr. Electric arc (21.5 V, 35A) was then applied to melt the materials into a silver shiny prill and this metal bead was flipped over and arc-melting again to ensure the homogeneity. The product was transferred and stored in an argon-filled glovebox before any characterization and measurement. This procedure was used to synthesize other compounds in $RECo_2$ ($RE = Pr, Tb, Y$ and Er) series. For Ru substitution, one has to change the loading ratio (1 : 0.5 : 1.5; RE: Ru : Co) and the rest of process is the same. Detail solid solution range between Ru and Co in Laves intermetallics is not included in this work but low Ru content sample $PrRu_{0.25}Co_{1.75}$ was also synthesized to investigate the influence of different Ru amount regarding electrocatalytic hydrogen evolution reaction (HER).

Material characterization and electrochemical measurement. The structural information and phase purity of the as-synthesized $RECo_2$, $RERu_{0.5}Co_{1.5}$ ($RE = Pr, Tb, Y$ and Er) and $PrRu_{0.25}Co_{1.75}$ were characterized by using Bruker X-ray powder diffractometer (D8 Advance, $Cu\ k\alpha_1$ 1.54056 Å). The scanning range was set from 20° to 60° and step size was fixed at 0.02°. JADE program was used to analyze diffraction patterns and full-pattern refinement was carried out to calculate unit cell parameters for each sample (Table S1). Additionally, the particle size, morphology and chemical composition of these Laves intermetallics were investigated by using field emission scanning electron microscope (FSEM, Model: S-4800) and energy dispersive spectrometer (EDS). The atomic ratio between the elements for all samples were listed in Table S2. X-ray photoelectron spectroscopy (XPS, Thermo Scientific, model: ESCALAB 250Xi) of as-synthesized materials were also acquired to analyze the valence states of Co and Ru atoms in materials. The reported photon energy of these spectrum was all calibrated based on the carbon internal standard. High-resolution transmission electron microscopy (HRTEM) images, STEM-EDX mapping image, were captured on a Tecnai G2 F30 transmission electron microscopy at an acceleration voltage of 300 kV.

In order to understand the effect of lanthanum contraction (crystal factor) and ligand effect (electronic factor) to HER performance of Laves intermetallics. $RECo_2$, $RERu_{0.5}Co_{1.5}$ ($RE = Pr, Tb, Y$ and Er) series and $PrRu_{0.25}Co_{1.75}$ were subjected to examining their HER activities in alkaline electrolyte (1.0 M KOH). Fresh samples in the argon-filled glovebox were ground into fine powder with mortar and pestle. These samples were then transferred into pellet press mold (ca. 50 mg) and dry pressing was implemented without any additives (e.g. nafion or carbon black). The pressed pellet was used as working electrode in a standard three electrodes system (Hg/HgO electrode as reference electrode and carbon rod as counter electrode) to measure corresponding electrochemical property in 1.0 M KOH solution (pH = 14) and potentials were converted to reversible hydrogen electrode (RHE) with 90% of ohmic potential drop losses (R_u).

Cyclic voltammetry with various scanning speeds was measured to calculate electrochemically active surface area (ECSA) and roughness factor (RF) for each sample. In details, we select potential range between -1.05 V and -1.00 V (V vs SCE; equal 0.008 V- 0.058 V vs RHE), then we run CV at different scan rate (20 mV/s, 40 mV/s, 60 mV/s, 80 mV/s, 100 mV/s). After acquire five CV curves, we can calculate capacitive current density (J/ cm^2) at mid-point potential (-1.025 V vs SCE) of CV scan simply by subtracting the negative current with positive current. The slope of linear fit of capacitive current and scan rate is the capacitance of electrocatalyst. The final step is to divide calculated capacitance with specific capacitance (40 $\mu F/ cm^2$) and one can obtain value of RF for electrocatalyst.

The linear sweep voltammograms (LSV; scan rate: 5 mV/ s) and RF normalized LSV curve were both included

to minimize the influence owing to the different surface area of electrode. The electrochemical behavior and HER performance of these materials show no noticeable difference between glass container and plastic container. In addition, these materials exhibit almost the same HER activities in the electrolyte w/wo purification.¹ This indicates that the influence of impurity (e.g. Fe and Si) may be limited and the change of the HER activity for these materials is intrinsic.

Theoretical calculation. To understand relationship between electronic structure and electrocatalytic HER activity of Laves intermetallics reported in this work, atomic simulation environment (ASE) software package equipped with GPAW calculator was used to calculate the adsorption energy (GH_{ad}) of H^* on hollow site that is composed of Co-Co/Ru bonds. Exchange-correlation energy was dealt with Revised Perdew-Burke-Ernzerhof (RPBE) functional in the system.² We choice Y element instead of other rare-earth metal for density functional theory (DFT) calculation of these Laves intermetallics because that calculation including f-electrons in the system is problematic. Considering the rare-earth metal in the structure of Laves intermetallics is mostly “space filler” and unlikely to be the active site for HER. Therefore, YCo_2 and $YRu_{0.25}Co_{1.75}$ were used to calculate their corresponding GH_{ad} instead of $PrCo_2$ and $PrRu_{0.25}Co_{1.75}$. The lattice constant was derived from full-pattern refinement (Table S1) of PXRD and (001) slab with 5 atomic layers was set to be the initial model. 15 Å vacuum spacing was inserted between each slab to avoid mutual interference. The top 3 layers including adsorbed H atom were allowed to relax during geometry optimization and final structure was determined when the maximum force of any atoms was lower than 0.05 eV \AA^{-1} .¹ Electronic energy was converted to free energy by including zero-point energy (ZPE) and entropy contribution of adsorbed H ($\Delta G = \Delta E + \Delta ZPE - T\Delta S$).

The model for YCo_2 is straightforward (space group Fd-3m), which there is only one Y atom (Wyckoff position 8b) and one Co atom (Wyckoff position 16c) in the asymmetric unit. The only one Co atom in the asymmetric unit of YCo_2 model, however, make it impossible to replace Co atom with Ru atom partially. Therefore, we lower the symmetry of YCo_2 and change the space group from Fd-3m to P2. This can generate six Y atoms and eight Co atoms in the asymmetric unit, while replacing one Co atom with Ru atom allows it to become $YRu_{0.25}Co_{1.75}$ (Ru : Co = 1 : 7). These models were used to calculate the total and partial density of states (TDOS and PDOS) by using TB-LMTO-ASA program.³ The bonding interactions (i.e. bonding scheme and character) of Co-Co/Ru bonds were also evaluated from crystal orbital Hamiltonian populations (COHP) to disclose the change of electronic structure due to Ru inclusion.

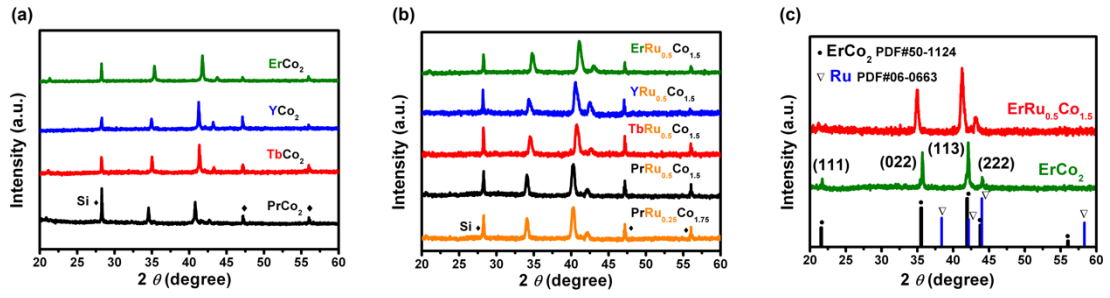


Figure S1. Experimental powder X-ray diffraction (PXRD) patterns of (a) $RECo_2$ and (b) $RERu_{0.5}Co_{1.5}$ ($RE = Pr, Tb, Y$ and Er) series with Si internal standard. (c) indexed PXRD of $ErCo_2$ and $ErRu_{0.5}Co_{1.5}$. JCPDS of Ru metal were included as well for comparison.

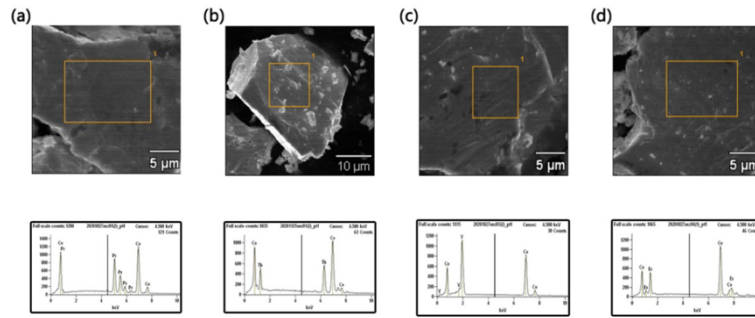


Figure S2. SEM image (top) and EDX spectrum (bottom) of (a) $PrCo_2$ (b) $TbCo_2$ (c) YCo_2 and (d) $ErCo_2$. The atomic ratio between rare-earth metal and Co for each sample derived from EDX analysis is tabulated in Table S2.

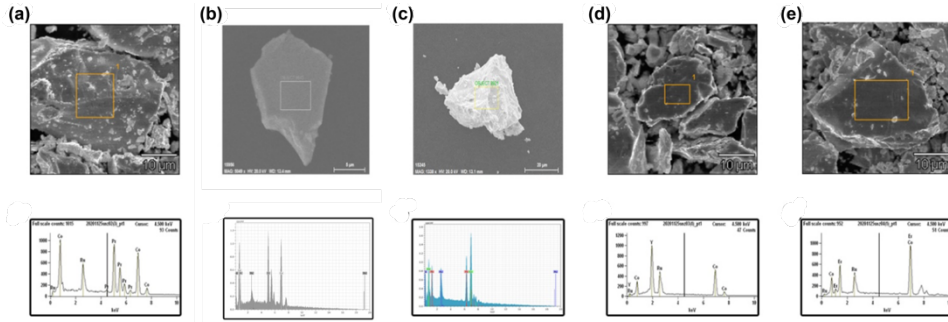


Figure S3. SEM image (top) and EDX spectrum (bottom) of (a) $PrRu_{0.5}Co_{1.5}$ (b) $PrRu_{0.25}Co_{1.75}$ (c) $TbRu_{0.5}Co_{1.5}$ (d) $YRu_{0.5}Co_{1.5}$ and (e) $ErRu_{0.5}Co_{1.5}$. The atomic ratio between rare-earth metal, Ru and Co for each sample derived from EDX analysis is tabulated in Table S3.

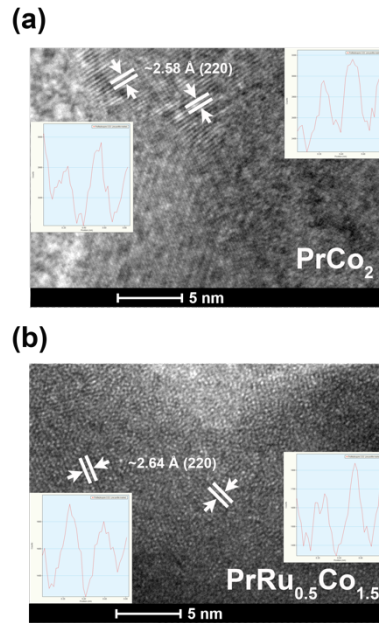


Figure S4. HR-TEM image of (a) PrCo_2 and (b) $\text{PrRu}_{0.5}\text{Co}_{1.5}$.

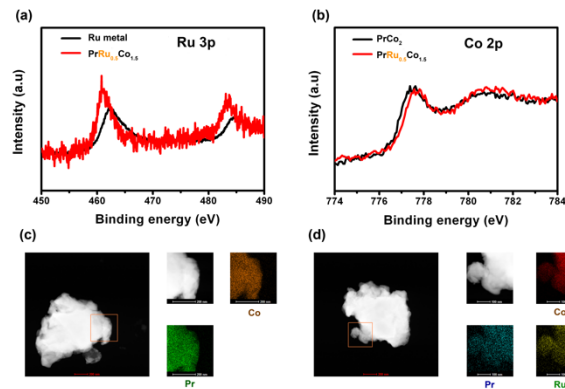


Figure S5. X-ray photoelectron spectrum (XPS) of (a) $\text{PrRu}_{0.5}\text{Co}_{1.5}$ and Ru metal in the Ru 3p regions. (b) XPS of PrCo_2 and $\text{PrRu}_{0.5}\text{Co}_{1.5}$ in the Co 2p regions. Scanning transmission electron microscopy (STEM) image and elemental mapping of (c) PrCo_2 and (b) $\text{PrRu}_{0.5}\text{Co}_{1.5}$.

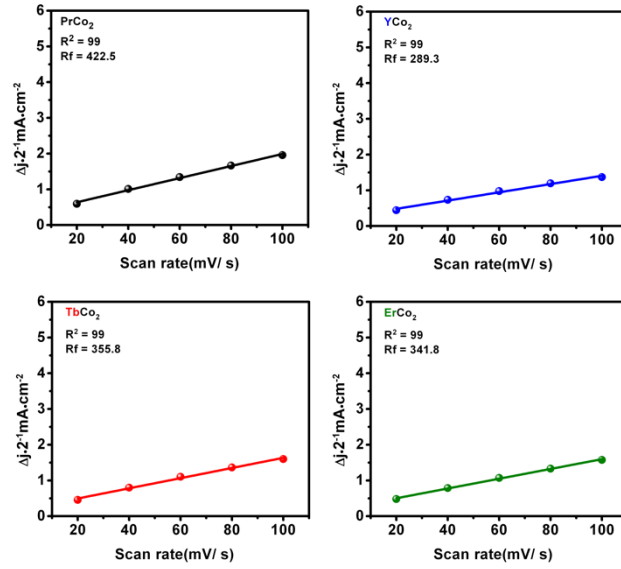


Figure S6. The linear regression slope derived from the cyclic voltammograms of RECo₂ (RE = Pr, Tb, Y and Er) series at 1.0 M KOH. Capacitive current density as a function of scan rate (20 – 100 mV/ s).

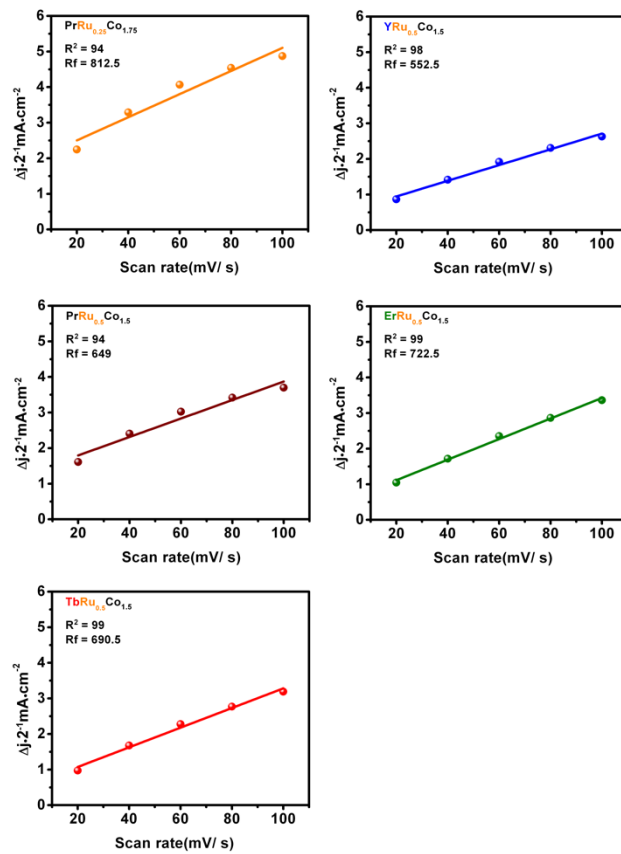


Figure S7. The linear regression slope derived from the cyclic voltammograms of RERu_{0.5}Co_{1.5} (RE = Pr, Tb, Y and Er) series and PrRu_{0.25}Co_{1.75} at 1.0 M KOH. Capacitive current density as a function of scan rate (20 – 100 mV/ s).

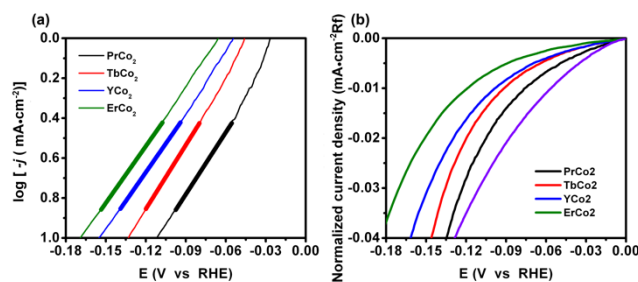


Figure S8. (a) Tafel plot and (b) normalized linear sweep voltammograms (LSV) based on roughness factor (Rf) for the hydrogen evolution reaction (HER) of $RECo_2$ ($RE = Pr, Tb, Y$ and Er) at 1.0 M KOH (scan rate: 5 mV/s).

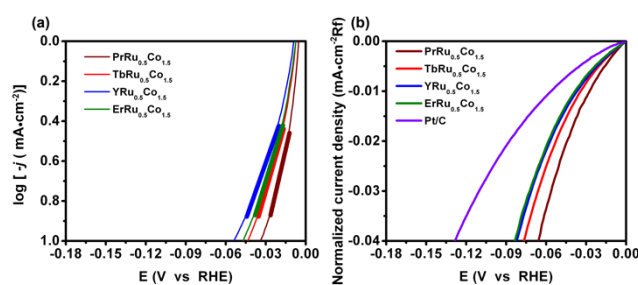


Figure S9. (a) Tafel plot and (b) normalized linear sweep voltammograms (LSV) based on roughness factor (Rf) for the hydrogen evolution reaction (HER) of $RERu_{0.25}Co_{1.5}$ ($RE = Pr, Tb, Y$ and Er) series at 1.0 M KOH (scan rate: 5 mV/s).

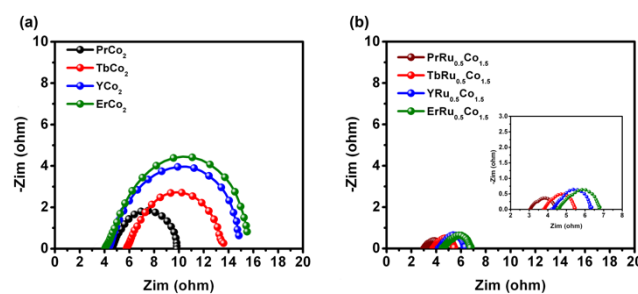


Figure S10. Electrochemical impedance spectroscopy (EIS) of $RECo_2$ and $RERu_{0.25}Co_{1.5}$ ($RE = Pr, Tb, Y$ and Er) in 1.0 M KOH at 1.578 V (V vs RHE).

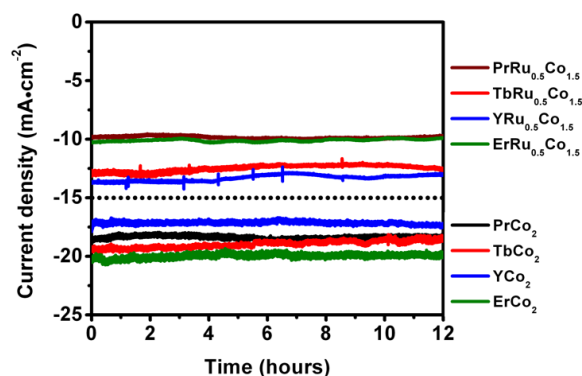


Figure S11. Chronoamperometry measurement of $RECo_2$ and $RERu_{0.25}Co_{1.5}$ ($RE = Pr, Tb, Y$ and Er) over a period of 12 hours in 1.0 M KOH.

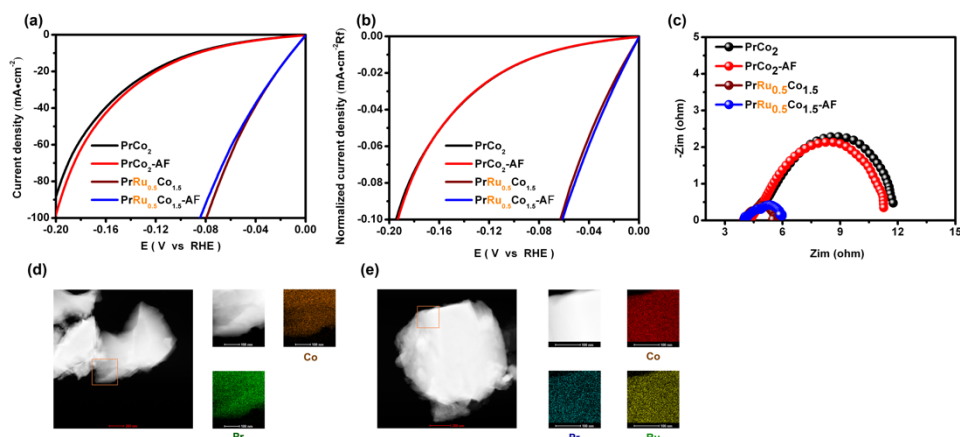


Figure S12. (a) linear sweep voltammograms (LSV), (b) normalized LSV based on roughness factor (RF), (c) electrochemical impedance spectroscopy (EIS) of PrCo₂ and PrRu_{0.5}Co_{1.5} before and after 1000 cycles of continuous operation toward hydrogen evolution reaction (HER). Scanning transmission electron microscopy (STEM) image and elemental mapping of PrCo₂ (d) and PrRu_{0.5}Co_{1.5} (e) after 1000 cycles of continuous operation.

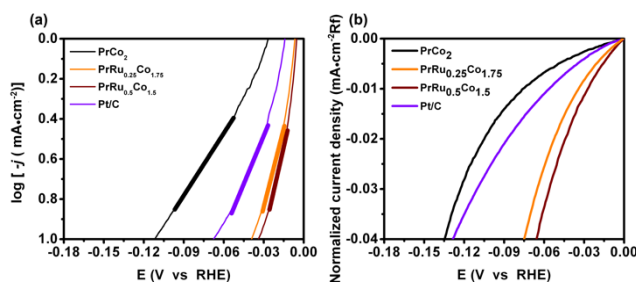


Figure S13. (a) Tafel plot and (b) normalized linear sweep voltammograms (LSV) based on roughness factor (Rf) for the hydrogen evolution reaction (HER) of PrCo₂, PrRu_{0.25}Co_{1.75}, PrRu_{0.5}Co_{1.5} and Pt/C at 1.0 M KOH (scan rate: 5 mV/s).

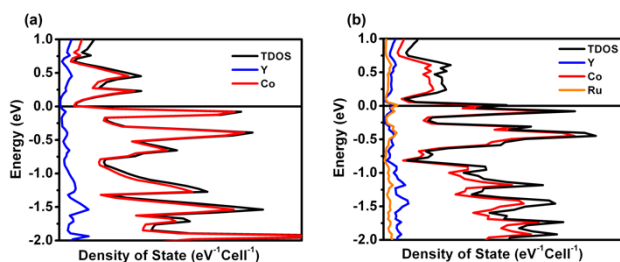


Figure S14. Calculated total density of states (DOS) and partial density of states (PDOS) curves for (a) YCo₂ and (b) YRu_{0.25}Co_{1.75}. Fermi level is set at the energy reference to 0 eV.

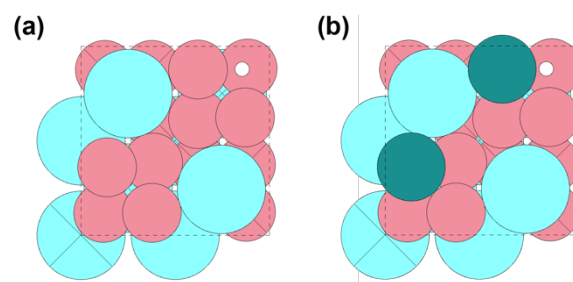


Figure S15. Model of (a) YCo_2 and (b) $\text{YRu}_{0.25}\text{Co}_{1.75}$ for the DFT calculation of hydrogen adsorption energy. The cyan and pink spheres represent Y and Co atoms, respectively. Ru atoms were shown in dark cyan sphere while H atoms are dyed in white color.

Table S1. Refined lattice constants for RECo_2 , $\text{RERu}_{0.5}\text{Co}_{1.5}$ ($\text{RE} = \text{Pr, Tb, Y and Er}$) and $\text{PrRu}_{0.25}\text{Co}_{1.75}$

formula	lattice constants	formula	lattice constants
	$a = b = c$		$a = b = c$
PrCo_2	7.2988(1)	$\text{PrRu}_{0.25}\text{Co}_{1.75}$	7.3358(1)
TbCo_2	7.2085(1)	$\text{PrRu}_{0.5}\text{Co}_{1.5}$	7.4023(1)
YCo_2	7.1973(1)	$\text{TbRu}_{0.5}\text{Co}_{1.5}$	7.3195(1)
ErCo_2	7.1366(1)	$\text{YRu}_{0.5}\text{Co}_{1.5}$	7.2906(1)
		$\text{ErRu}_{0.5}\text{Co}_{1.5}$	7.2490(1)

Table S2. Atomic ratio of RECo_2 ($\text{RE} = \text{Pr, Tb, Y and Er}$) from EDX analysis.

	element	atomic ratio (%)
PrCo_2	Pr	29.53
	Co	70.47
TbCo_2	Tb	36.01
	Co	63.99
YCo_2	Y	30.11
	Co	69.87
ErCo_2	Er	29.5
	Co	70.5

Table S3. Atomic ratio of $\text{PrRu}_{0.25}\text{Co}_{1.75}$ and $\text{RERu}_{0.5}\text{Co}_{1.5}$ ($\text{RE} = \text{Pr, Tb, Y and Er}$) from EDX analysis.

	element	atomic ratio (%)
$\text{PrRu}_{0.25}\text{Co}_{1.75}$	Pr	36.68
	Ru	7.60
	Co	55.72
$\text{PrRu}_{0.5}\text{Co}_{1.5}$	Pr	36.75
	Ru	12.71
	Co	47.82
$\text{TbRu}_{0.5}\text{Co}_{1.5}$	Tb	32.36
	Ru	15.21
	Co	52.21
$\text{YRu}_{0.5}\text{Co}_{1.5}$	Y	28.84
	Ru	19.39
	Co	51.77
$\text{ErRu}_{0.5}\text{Co}_{1.5}$	Er	32.18
	Ru	15.86
	Co	51.96

REFERENCES

- 1 L. Trotochaud, S. L. Young, J. K. Ranney and S. W. Boettcher, *J. Am. Chem. Soc.*, 2014, **136**, 6744-6753.
- 2 A. H. Larsen, J. J. Mortensen, J. Blomqvist, I. E. Castelli, R. Christensen, M. Dulak, J. Friis, M. N. Groves, B. Hammer, C. Hargus, E. D. Hermes, P. C. Jennings, P. B. Jensen, J. Kermode, J. R. Kitchin, E. L. Kolsbjerg, J. Kubal, K. Kaasbjerg, S. Lysgaard, J. B. Maronsson, T. Maxson, T. Olsen, L. Pastewka, A. Peterson, C. Rostgaard, J. Schiøtz, O. Schutt, M. Strange, K. S. Thygesen, T. Vegge, L. Vilhelmsen, M. Walter, Z. H. Zeng, K. W. Jacobsen, *J. Am. Chem. Soc.*, 2017, **29**, 273002; (b) J. Enkovaara, C. Rostgaard, J. J. Mortensen, J. Chen, M. Dulak, L. Ferrighi, J. Gavnholt, C. Glinsvad, V. Haikola, H. A. Hansen, H. H. Kristoffersen, M. Kuisma, A. H. Larsen, L. Lehtovaara, M. Ljungberg, O. Lopez-Acevedo, P. G. Moses, J. Ojanen, T. Olsen, V. Petzold, N. A. Romero, J. Stausholm-Møller, M. Strange, G. A. Tritsarlis, M. Vanin, M. Walter, B. Hammer, H. Häkkinen, G. K. H. Madsen, R. M. Nieminen, J. K. Nørskov, M. Puska, T. T. Rantala, J. Schiøtz, K. S. Thygesen and K. W. Jacobsen, *J. Phys.: Condens. Matter*, 2010, **22**, 253202; (c) J. J. Mortensen, L. B. Hansen and K. W. Jacobsen, *Phys. Rev. B*, 2005, **71**, 035109; (d) B. Hammer, L. B. Hansen and J. K. Nørskov, *Phys. Rev. B*, 1999, **59**, 7413-7421; (e) J. J. Mortensen, L. B. Hansen and K. W. Jacobsen, *Physical Review B*, 2005, **71**; (f) J. Enkovaara, C. Rostgaard, J. J. Mortensen, J. Chen, M. Dulak, L. Ferrighi, J. Gavnholt, C. Glinsvad, V. Haikola, H. A. Hansen, H. H. Kristoffersen, M. Kuisma, A. H. Larsen, L. Lehtovaara, M. Ljungberg, O. Lopez-Acevedo, P. G. Moses, J. Ojanen, T. Olsen, V. Petzold, N. A. Romero, J. Stausholm-Møller, M. Strange, G. A. Tritsarlis, M. Vanin, M. Walter, B. Hammer, H. Häkkinen, G. K. H. Madsen, R. M. Nieminen, J. Nørskov, M. Puska, T. T. Rantala, J. Schiøtz, K. S. Thygesen and K. W. Jacobsen, *J. Phys.: Condens. Matter*, 2010, **22**; (g) A. H. Larsen, J. J. Mortensen, J. Blomqvist, I. E. Castelli, R. Christensen, M. Dulak, J. Friis, M. N. Groves, B. Hammer, C. Hargus, E. D. Hermes, P. C. Jennings,

P. B. Jensen, J. Kermode, J. R. Kitchin, E. L. Kolsbjerg, J. Kubal, K. Kaasbjerg, S. Lysgaard, J. B. Maronsson, T. Maxson, T. Olsen, L. Pastewka, A. Peterson, C. Rostgaard, J. Schiotz, O. Schutt, M. Strange, K. S. Thygesen, T. Vegge, L. Vilhelmsen, M. Walter, Z. H. Zeng and K. W. Jacobsen, *J. Phys.: Condens. Matter*, 2017, **29**.

- 3 (a) L. Trotochaud, S. L. Young, J. K. Ranney and S. W. Boettcher, *J. Am. Chem. Soc.*, 2014, **136**, 6744-6753; (b) TB-LMTO-ASAP program, version 4.7, Max-Planck-Institut für Festkörperforschung, Stuttgart, Germany, 1998.